Monthly Notices of the ROYAL ASTRONOMICAL SOCIETY

MNRAS **464,** 1466–1473 (2017) doi:10.1093/mnras/stw2467
Advance Access publication 2016 September 28

BAT AGN Spectroscopic Survey – III. An observed link between AGN Eddington ratio and narrow-emission-line ratios

Kyuseok Oh,[1⋆] Kevin Schawinski,[1⋆] Michael Koss,[1⋆†] Benny Trakhtenbrot,[1‡] Isabella Lamperti,[1] Claudio Ricci,[2] Richard Mushotzky,[3] Sylvain Veilleux,[3] Simon Berney,[1] D. Michael Crenshaw,[4] Neil Gehrels,[5] Fiona Harrison,[6] Nicola Masetti,[7,8] Kurt T. Soto,[1] Daniel Stern,[9] Ezequiel Treister[2] and Yoshihiro Ueda[10]

[1]*Institute for Astronomy, Department of Physics, ETH Zurich, Wolfgang-Pauli-Strasse 27, CH-8093 Zurich, Switzerland*
[2]*Instituto de Astrofísica, Facultad de Física, Pontificia Universidad Católica de Chile, Casilla 306, Santiago 22, Chile*
[3]*Astronomy Department and Joint Space-Science Institute, University of Maryland, College Park, MD 20742, USA*
[4]*Department of Physics and Astronomy, Georgia State University, Astronomy Offices, One Park Place South SE, Suite 700, Atlanta, GA 30303, USA*
[5]*NASA Goddard Space Flight Center, Greenbelt, MD 20771, USA*
[6]*Cahill Center for Astronomy and Astrophysics, California Institute of Technology, Pasadena, CA 91125, USA*
[7]*INAF – Istituto di Astrofisica Spaziale e Fisica Cosmica di Bologna, via Gobetti 101, 40129 Bologna, Italy*
[8]*Departamento de Ciencias Físicas, Universidad Andrés Bello, Fernández Concha 700, Las Condes 7591583, Santiago, Chile*
[9]*Jet Propulsion Laboratory, California Institute of Technology, 4800 Oak Grove Drive, MS 169-224, Pasadena, CA 91109, USA*
[10]*Department of Astronomy, Kyoto University, Kyoto 606-8502, Japan*

Accepted 2016 September 27. Received 2016 September 24; in original form 2016 June 21

ABSTRACT

We investigate the observed relationship between black hole mass ($M_{\rm BH}$), bolometric luminosity ($L_{\rm bol}$) and Eddington ratio ($\lambda_{\rm Edd}$) with optical emission-line ratios ([N II] λ6583/Hα, [S II] $\lambda\lambda$6716, 6731/Hα, [O I] λ6300/Hα, [O III] λ5007/Hβ, [Ne III] λ3869/Hβ and He II λ4686/Hβ) of hard X-ray-selected active galactic nuclei (AGN) from the BAT AGN Spectroscopic Survey. We show that the [N II] λ6583/Hα ratio exhibits a significant correlation with $\lambda_{\rm Edd}$ ($R_{\rm Pear} = -0.44$, p-value $= 3 \times 10^{-13}$, $\sigma = 0.28$ dex), and the correlation is not solely driven by $M_{\rm BH}$ or $L_{\rm bol}$. The observed correlation between [N II] λ6583/Hα ratio and $M_{\rm BH}$ is stronger than the correlation with $L_{\rm bol}$, but both are weaker than the $\lambda_{\rm Edd}$ correlation. This implies that the large-scale narrow lines of AGN host galaxies carry information about the accretion state of the AGN central engine. We propose that [N II] λ6583/Hα is a useful indicator of Eddington ratio with 0.6 dex of rms scatter, and that it can be used to measure $\lambda_{\rm Edd}$ and thus $M_{\rm BH}$ from the measured $L_{\rm bol}$, even for high-redshift obscured AGN. We briefly discuss possible physical mechanisms behind this correlation, such as the mass–metallicity relation, X-ray heating, and radiatively driven outflows.

Key words: black hole physics – galaxies: active – galaxies: nuclei – quasars: general.

1 INTRODUCTION

Nebular emission lines are a powerful tool for diagnosing the physical state of ionized gas and studying central nuclear activity. Optical emission-line ratios can be used to discriminate between emission from the star formation in galaxies and harder radiation such as from the central nuclear activity around a supermassive black hole (e.g. Baldwin, Phillips & Terlevich 1981; Veilleux & Osterbrock 1987; Kewley et al. 2001; Kauffmann et al. 2003). Compared to star-forming galaxies, active galactic nuclei (AGN) produce greater numbers of higher energy photons [e.g. ultraviolet (UV) and X-rays] and therefore drive higher ratios of the collisionally excited forbidden lines compared to the photoionization-induced Balmer emission lines. Although such line ratios provide useful AGN diagnostics, even for obscured AGN (Reyes et al. 2008; Yuan, Strauss & Zakamska 2016), they may not be effective in selecting all heavily obscured AGN and/or AGN that lack significant amounts of low-density gas (Elvis et al. 1981; Iwasawa et al. 1993; Griffiths et al. 1995; Barger et al. 2001; Comastri et al. 2002; Rigby et al. 2006; Caccianiga et al. 2007).

⋆ E-mail: ohk@phys.ethz.ch (KO); kevin.schawinski@phys.ethz.ch (KS); mike.koss@phys.ethz.ch (MK)
† Ambizione fellow.
‡ Zwicky fellow.

With the recent advent of hard X-ray (>10 keV) facilities, such as *INTEGRAL* (Winkler et al. 2003), *Swift* (Gehrels et al. 2004), and *NuSTAR* (Harrison et al. 2013), it is now possible to study samples of AGN that are less biased to obscuration and include even Compton-thick sources ($N_{\rm H} > 10^{24}$ cm^{-2}, Ricci et al. 2015; Koss et al. 2016). In particular, the Burst Alert Telescope (BAT, Barthelmy et al. 2005) on board the *Swift* satellite has been observing the sky in the 14–195 keV energy band since 2005, reaching sensitivities of 1.3×10^{-11} erg cm^{-2} s^{-1} over 90 per cent of the sky. The 70-month *Swift*-BAT all-sky hard X-ray survey[1] detected 1210 objects, of which 836 are AGN (Baumgartner et al. 2013). While the BAT detection is relatively unabsorbed up to Compton-thick levels (e.g. $N_{\rm H} < 10^{24}$ cm^{-2}, Koss et al. 2016), heavily Compton-thick AGN ($N_{\rm H} > 10^{25}$ cm^{-2}) are missed by X-ray surveys but may sometimes be detected using optical emission-line diagnostics and strong [O III] λ5007 emission lines (e.g. Maiolino et al. 1998).

The relationship between Eddington ratio ($\lambda_{\rm Edd} \equiv L/L_{\rm Edd}$, where $L_{\rm Edd} \equiv 1.3 \times 10^{38} M_{\rm BH}/{\rm M}_{\odot}$) and the position of AGN in emission-line diagrams is an important topic of study because of the difficulty in measuring black hole mass ($M_{\rm BH}$) from velocity dispersion in high-redshift AGN. Kewley et al. (2006) investigated host properties of nearby emission-line galaxies ($0.04 < z < 0.1$) from the Sloan Digital Sky Survey (SDSS). They found that the $\lambda_{\rm Edd}$ (inferred from $L_{\rm [OIII]}/{\sigma_\star}^4$, where $\sigma_\star$ is a stellar velocity dispersion) shows an increase with ϕ, a measure of distance from the low-ionization nuclear emission-line region (LINER) regime in the [O III] λ5007/Hβ versus [O I] λ6300/Hα diagram. Similarly, an SDSS study of unobscured AGN by Stern & Laor (2013) found a dependence of emission-line diagnostics on the $\lambda_{\rm Edd}$. However, the estimation of $\lambda_{\rm Edd}$ and the introduced relationship between the angle ϕ and $L_{\rm [OIII]}/{\sigma_\star}^4$ were both dependent on the strength of [O III] λ5007. Also, the previous studies did not take into account X-ray selection focusing on the large sample of optically selected AGN. Both highly ionized optical emission lines and X-rays are thought to be a measure of the AGN bolometric luminosity. However, hard X-rays are less biased against dust obscuration and the contribution from star-forming activity than optical emission lines.

The BAT AGN Spectroscopic Survey (BASS) Data Release 1 (Koss et al., submitted) compiled 642 optical spectra of nearby AGN ($\langle z \rangle \sim 0.05$) from public surveys (SDSS and 6dF; Abazajian et al. 2009; Jones et al. 2009; Alam et al. 2015) and dedicated follow-up observations (e.g. from telescopes at the Kitt Peak, Gemini, Palomar, and SAAO observatories). The data release provided emission-line measurements as well as $M_{\rm BH}$ and $\lambda_{\rm Edd}$ estimates for the majority of obscured and unobscured AGN (74 per cent, 473/642), including 340 AGN with $M_{\rm BH}$ measurements reported for the first time.

In this paper, we use the BASS measurements to investigate the observed relationship between black hole mass ($M_{\rm BH}$), bolometric luminosity ($L_{\rm bol}$), and Eddington ratio ($\lambda_{\rm Edd}$) with optical emission-line ratios ([N II] λ6583/Hα, [S II] λλ6716, 6731/Hα, [O I] λ6300/Hα, [O III] λ5007/Hβ, [Ne III] λ3869/Hβ, and He II λ4686/Hβ) for both obscured and unobscured AGN.

We assume a cosmology with $h = 0.70$, $\Omega_{\rm M} = 0.30$, and $\Omega_\Lambda = 0.70$ throughout this work.

2 SAMPLE SELECTION, DATA, AND MEASUREMENTS

In this section, we briefly summarize the measurement procedures for optical emission lines, $M_{\rm BH}$, and $\lambda_{\rm Edd}$. The BASS DR1 measured nebular emission-line strengths by performing a power-law fit with Gaussian components to model the continuum and emission lines. For unobscured AGN, two Gaussian components are allowed in the Hα and Hβ emission-line regions to account for both broad [full width at half-maximum (FWHM) > 1000 km s^{-1}] and narrow (FWHM < 1000 km s^{-1}) components. When broad Hβ is detected, $M_{\rm BH}$ is measured using the single-epoch method following Trakhtenbrot & Netzer (2012). If no broad Hβ is detected, $M_{\rm BH}$ is measured based on the linewidth and luminosity of broad Hα (equation 9 from Greene & Ho 2005). For obscured AGN, the estimation of $M_{\rm BH}$ relies on the close correlations between $M_{\rm BH}$ and the stellar velocity dispersion ($\sigma_\star$, e.g. Kormendy & Ho 2013). Stellar velocity dispersion is derived from the penalized pixel-fitting method (pPXF, Cappellari & Emsellem 2004) by implementing a modified version of the masking procedure introduced for the analysis of SDSS DR7 (Abazajian et al. 2009) galaxy spectra (the OSSY catalogue,[2] Sarzi et al. 2006; Oh et al. 2011, 2015).

Since the obscuration mostly affects the estimation of $L_{\rm bol}$ for Compton-thick AGN ($N_{\rm H} > 10^{24}$ cm^{-2}), we estimated $L_{\rm bol}$ from the intrinsic (i.e. absorption and k-corrected) 14–150 keV luminosities reported in Ricci et al. (2015) and Ricci et al. (in preparation), transforming them into 14–195 keV luminosities assuming a power-law continuum with a photon index of Gamma = 1.9. After converting the 14–195 keV luminosity into the intrinsic 2–10 keV luminosity by following the procedure described by Rigby, Diamond-Stanic & Aniano (2009), we applied the median bolometric correction introduced by Vasudevan et al. (2009). It is noteworthy to mention that the estimation of $L_{\rm bol}$ comes solely from the hard X-ray band (14–195 keV) and its constant conversion factor ($k = 8$). We briefly discuss the effect of the estimation of different $L_{\rm bol}$ in Section 3. We then combined the measured $M_{\rm BH}$ with the $L_{\rm bol}$ to calculate $\lambda_{\rm Edd}$ ($\lambda_{\rm Edd} \equiv L_{\rm bol}/L_{\rm Edd}$), assuming $L_{\rm Edd} \equiv 1.3 \times 10^{38} (M_{\rm BH}/{\rm M}_{\odot})$. For more details, refer to the first data release (Koss et al., submitted).

We focus on the subsample of the 642 optical spectra from the BASS DR1. We consider only non-beamed AGN, which were selected by cross-matching the BASS sources with the Roma blazar catalogue (BZCAT) v5.0 (Massaro et al. 2009). We then restricted our samples to redshifts of $0.01 < z < 0.40$ to have coverage of the Hβ and Hα regions. Berney et al. (2015) investigated the effect of slit size for the BASS DR1 sources and showed that the ratio between extinction-corrected L[O III] and $L_{\rm 14-195keV}$ is constant when excluding the nearest galaxies ($z < 0.01$), whereas the scatter slightly decreases towards larger slit sizes. We used the same redshift range as followed in this approach. However, it should be noted that the aperture effect does not change our results shown in Section 3. We tested whether sources with large physical coverage (>2 kpc) still found a significant correlation in a smaller sample size, suggesting that slit size is not important for this study. We also selected only spectral fits with a good quality as listed in the DR1 tables (Koss et al., submitted). We note that sources with spectra taken from the 6dF Galaxy Survey (Jones et al. 2009) are used only to derive emission-line ratios and to measure stellar velocity dispersions (e.g. Campbell et al. 2014) due to the lack of flux calibration, as necessary for broad-line black hole mass measurements.

[1] http://heasarc.gsfc.nasa.gov/docs/swift/results/bs70mon/

[2] http://gem.yonsei.ac.kr/ossy/

Table 1. Bayesian linear regression fit.

Line ratio (1)	N (2)	α (3)	β (4)	RMSD (5)	$R_{\rm Pear}$ (p-value) (6)	$R_{\rm Pear,unobs}$ (p-value) (7)	$R_{\rm Pear,obs}$ (p-value) (8)
[N II] λ6583/Hα	297	-0.42 ± 0.04	-0.19 ± 0.02	0.28	-0.44 (3×10^{-13})	-0.34 (0.000 02)	-0.28 (0.001 28)
[S II] λλ6716, 6731/Hα	288	-0.48 ± 0.03	-0.11 ± 0.02	0.25	-0.29 (9×10^{-7})	-0.26 (0.000 80)	0.11 (0.561 80)
[O I] λ6300/Hα	205	···	···	···	(0.033 14)	(0.027 77)	(0.364 99)
[O III] λ5007/Hβ	286	···	···	···	(0.328 77)	(0.384 56)	(0.348 75)
[Ne III] λ3869/Hβ	125	···	···	···	(0.871 41)	(0.381 63)	(0.786 29)
He II λ4686/Hβ	107	···	···	···	(0.875 16)	(0.564 90)	(0.085 83)

Notes. (1) Optical emission-line ratio; (2) size of sample; (3) intercept; (4) slope; (5) rms deviation; (6) Pearson R coefficient and p-value; (7) Pearson R coefficient and p-value for unobscured AGN; and (8) Pearson R coefficient and p-value for obscured AGN.

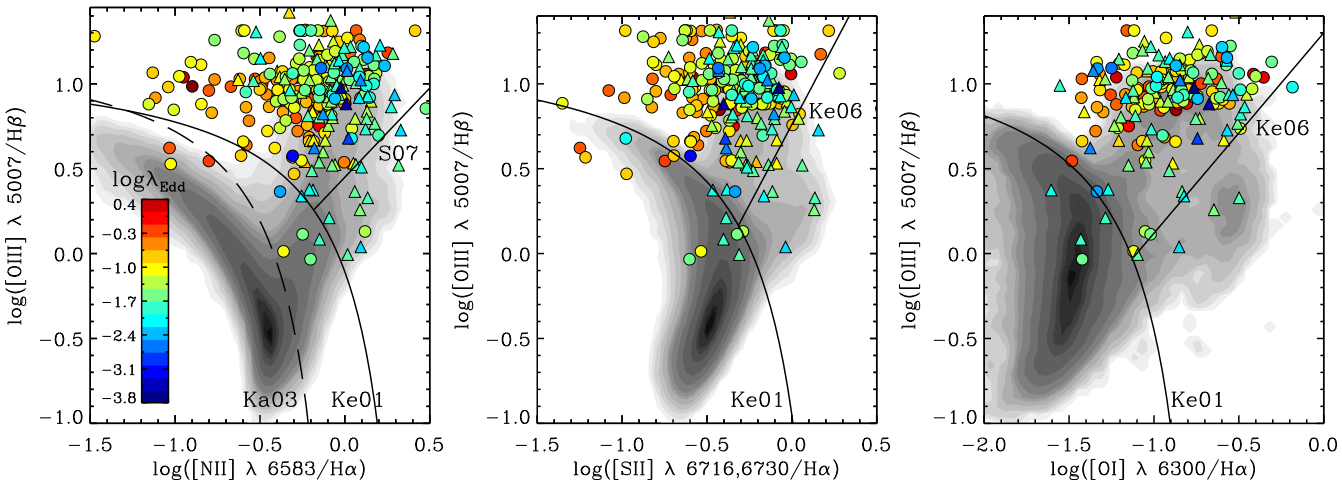

Figure 1. Emission-line diagnostic diagrams for the BASS sources with signal-to-noise ratio (S/N) > 3. Left-hand panel: [N II] λ6583/Hα versus [O III] λ5007/Hβ diagnostic diagram. Colour filled circles and triangles indicate type 1 AGN (including type 1.9) and type 2 AGN, respectively. The empirical star formation curve obtained from Kauffmann et al. (2003) (dashed curve) and the theoretical maximum starburst model of Kewley et al. (2001) (solid curve) are used. The solid straight line is the empirical demarcation of Schawinski et al. (2007) distinguishing the Seyfert AGN from the LINERs. The Eddington ratio of BASS sources is shown with colour-filled dots. Middle panel: [S II] λλ6716, 6731/Hα versus [O III] λ5007/Hβ diagnostic diagram. Right-hand panel: [O I] λ6300/Hα versus [O III] λ5007/Hβ diagnostic diagram. Demarcation lines from Kewley et al. (2001, 2006) are used. In all panels, we also show more than 180 000 SDSS emission-line galaxies with filled contours chosen from the OSSY catalogue ($z < 0.2$) with S/N > 3 for [N II] λ6583, Hα, [O III] λ5007, Hβ, [SII] λ6716, [SII] λ6731, and [OI] λ6300.

Samples sizes for each emission-line ratio used in this paper are listed in Table 1.

3 RELATIONS BETWEEN OPTICAL EMISSION-LINE RATIOS AND BASIC AGN PROPERTIES

Fig. 1 shows the emission-line diagnostic diagrams for the BASS sources according to $\lambda_{\rm Edd}$ (colour-coded). The majority of the BASS sources (>90 per cent) are found in the Seyfert region in each panel.

In order to study the statistical significance of any correlations with $\lambda_{\rm Edd}$, we show optical emission-line ratios as a function of $\lambda_{\rm Edd}$ in Fig. 2. We performed a Bayesian linear regression fit (equation 1) to all points using the method of Kelly (2007), which accounts for measurement errors in both axes. The relation between $\lambda_{\rm Edd}$ and optical emission-line ratio (black solid line in Fig. 2) is determined by taking the median of 10 000 draws from the posterior probability distribution of the converged parameters (intercept and slope). The errors of intercept and slope are reported from a 1σ confidence ellipse. The root-mean-square (rms) deviation is shown with black dotted lines in each panel.

$$\log(F_{\rm line}/F_{\rm Balmer}) = \alpha + \beta \log \lambda_{\rm Edd}. \quad (1)$$

The values of α (intercept), β (slope), Pearson correlation coefficient, rms deviation, and p-value are summarized in Table 1.

We find that the $\lambda_{\rm Edd}$ is significantly anticorrelated with optical emission-line ratios for both the [N II] λ6583/Hα and the [S II] λλ6716, 6731/Hα ratios but not for the other line ratios. The larger the $\lambda_{\rm Edd}$, the smaller the line ratio of [N II] λ6583/Hα and [S II] λλ6716, 6731/Hα. We find that the Pearson R coefficient and p-value of the anticorrelation between [N II] λ6583/Hα and $\lambda_{\rm Edd}$ are -0.44 and 3×10^{-13}, respectively, with 0.28 dex of rms deviation. We also found a significantly anticorrelated relationship for both the [N II] λ6583/Hα and [S II] λλ6716, 6731/Hα ratios with a more stringent S/N cut of optical emission lines (>10). AGN variability may induce the scatter shown in the anticorrelation between [N II] λ6583/Hα and $\lambda_{\rm Edd}$. Since the X-ray emission that we used to derive $L_{\rm bol}$ and $\lambda_{\rm Edd}$ has different time-scales compared to optical narrow emission lines, a scatter around the anticorrelation can be explained (Mushotzky, Done & Pounds 1993; Schawinski et al. 2015). Also, differences in metallicities and/or structures of the narrow-line regions may contribute to the scatter shown above. In order to quantitatively investigate if the $\lambda_{\rm Edd}$ shows a stronger anticorrelation with [N II] λ6583/Hα or with [S II] λλ6716, 6731/Hα, we run a z-test based on the two Pearson correlation coefficients (Fisher r-to-z transformation). The p-value (0.019) suggests that

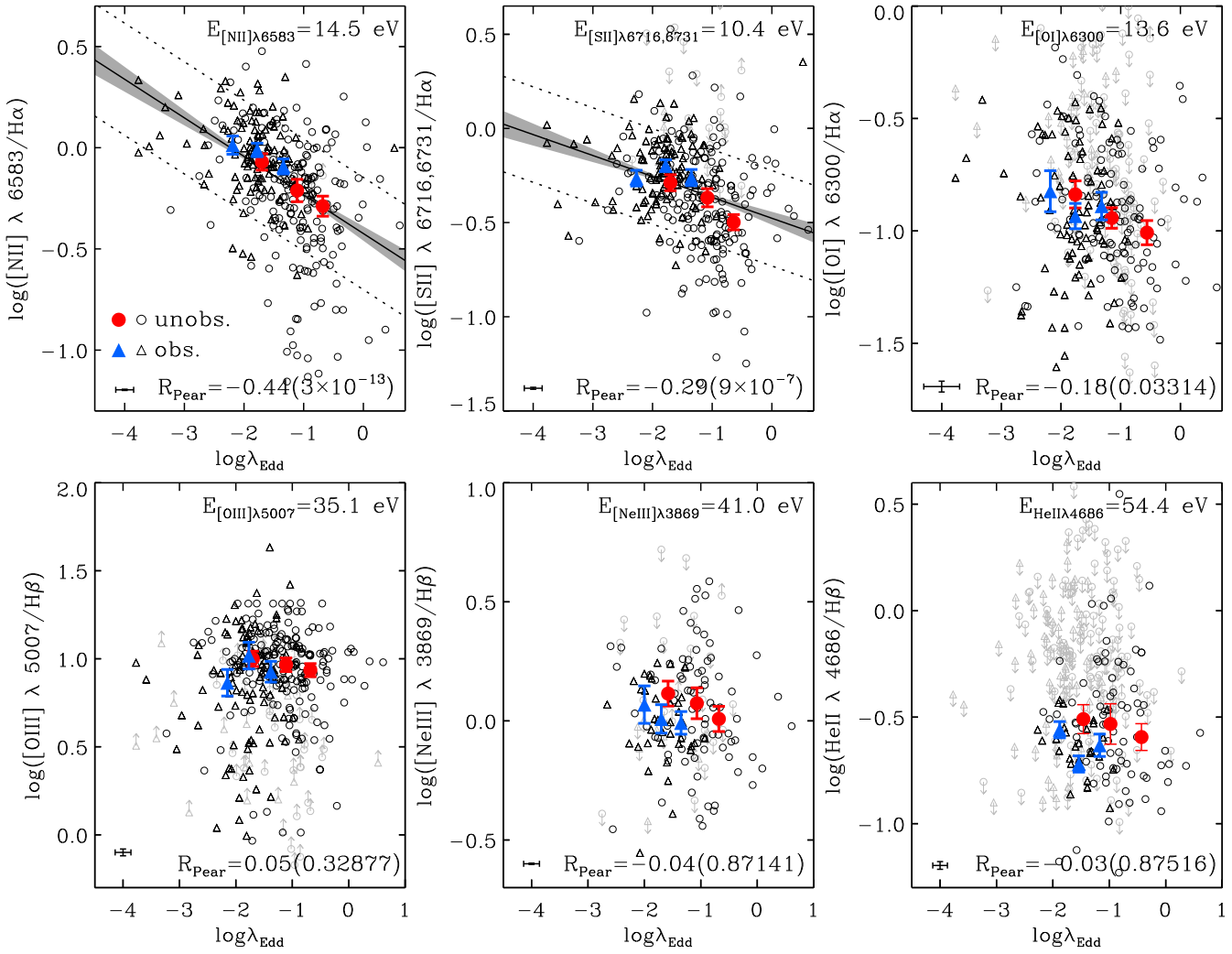

Figure 2. Optical emission-line ratio versus Eddington ratio diagram. Black open circles and triangles indicate type 1 AGN (including type 1.9) and type 2 AGN, respectively. Median at each bin is shown with colour-filled symbols. Bin size is determined to have at least 10 sources. Black solid lines indicate the Eddington ratio–optical emission-line ratio relations (equation 1). The grey-shaded regions account for the errors in the slope and intercept of the relation. The rms deviation is shown with dotted lines. An error bar in the bottom left-hand corner of each panel indicates typical uncertainties in Eddington ratio and optical emission-line ratio. The ionization potential for each emission line is shown in the legends. Also, Pearson correlation coefficients and p-values are shown in the bottom right-hand corner of each panel. An emission-line detection at S/N < 3 (upper or lower limit) is shown with grey symbols.

[N II] λ6583/Hα shows a significantly stronger anticorrelation than [S II] λλ6716, 6731/Hα with $\lambda_{\rm Edd}$.

Moreover, we also find that the observed anticorrelation between [N II] λ6583/Hα and $\lambda_{\rm Edd}$ is valid for obscured AGN (blue filled triangles in Fig. 2) as well as unobscured AGN (red filled circles in Fig. 2). The Pearson R coefficient and p-value for obscured AGN are −0.28 and 0.00128, respectively. For unobscured AGN, we report −0.34 and 0.00002 as the Pearson R coefficient and p-value. We report that $\lambda_{\rm Edd}$ can be estimated from the measured [N II] λ6583/Hα ratio as follows, with 0.6 dex of rms deviation:

$$\log \lambda_{\rm Edd} = (-1.52 \pm 0.04) + (-1.00 \pm 0.13) \times \log([{\rm N\,II}]\lambda 6583/{\rm H}\alpha). \quad (2)$$

Another way to study the location on the emission-line diagnostic diagram is to measure the shortest distance from the star-forming and LINER lines in [N II] λ6583/Hα. The $\lambda_{\rm Edd}$ distribution shown in the [N II] λ6583/Hα emission-line diagnostic diagram (left-hand panel of Fig. 1) enables us to infer that AGN falling in the Seyfert region exhibit different $\lambda_{\rm Edd}$ according to their location, i.e. combinations of emission-line ratios. We define the distance between the location of a given object and the empirical demarcation line of Schawinski et al. (2007) ($d_{\rm LINER}$) and the theoretical maximum starburst model of Kewley et al. (2001) ($d_{\rm SF}$). The separation between the Seyfert and LINER was obtained by a visual determination based on the [N II] λ6583/Hα versus [O III] λ5007/Hβ diagram for nearly 50 000 nearby SDSS galaxies ($0.05 < z < 0.10$, Schawinski et al. 2007). For Seyferts and LINERs classified using the [S II] λλ6716, 6731/Hα and [O I] λ6300/Hα diagrams, the authors determined the demarcation line in the [N II] λ6583/Hα diagram. In particular, we measured $d_{\rm SF}$ by moving the demarcation line of Kewley et al. (2001) in parallel with the original one until it matches the location of the given object. The measured distance, $d_{\rm LINER}$, that originated from optical emission-line ratios, which depict the physical state of the innermost region of the galaxy, is a function of the $\lambda_{\rm Edd}$ (middle panel in Fig. 3). We report the Pearson R coefficient and p-value for $d_{\rm LINER}$ and log $\lambda_{\rm Edd}$ with 0.31 and 5×10^{-7}, whereas $d_{\rm SF}$ shows less significant statistics ($R_{\rm Pear} = -0.18$, p-value $= 0.00423$), suggesting

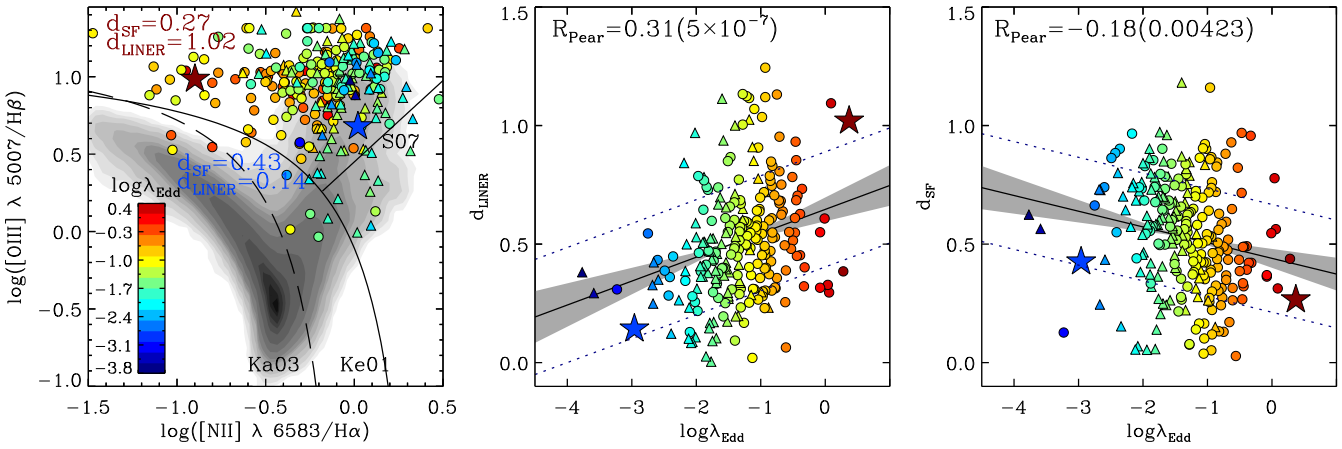

Figure 3. $d_{\rm LINER}$ and $d_{\rm SF}$ as a function of Eddington ratio. The left-hand panel illustrates distances of two examples (star symbols) with corresponding colour-coded Eddington ratios, as in Fig. 1. The middle and right-hand panels show the $d_{\rm LINER}$ and $d_{\rm SF}$ distributions, respectively. The Bayesian linear regression fit, errors in the slope, intercept of the fit, and rms deviation are shown with black straight lines, grey-shaded regions, and dotted lines, respectively, as in Fig. 2.

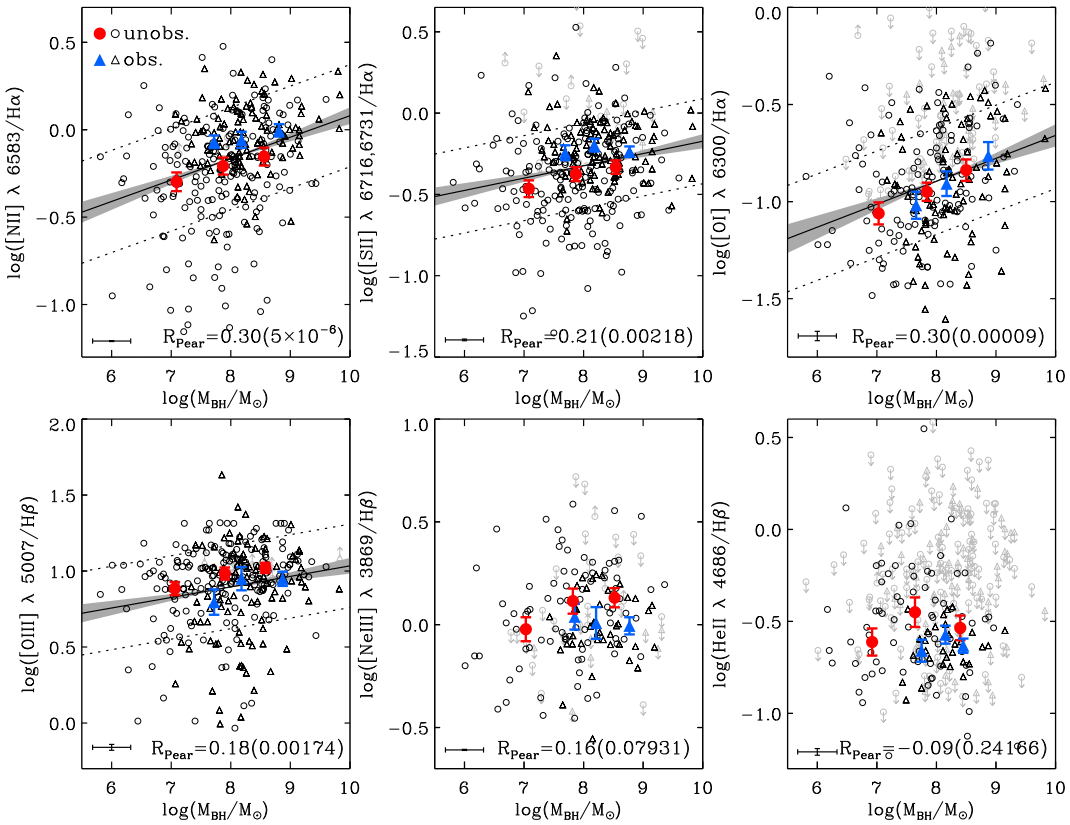

Figure 4. Optical emission-line ratio versus black hole mass. The format is the same as that of Fig. 2.

that $\lambda_{\rm Edd}$ is less likely a function of $d_{\rm SF}$. We also ran a test to see if sources with extreme $\lambda_{\rm Edd}$ were driving correlations we found. For this test, we used a limited range of $\lambda_{\rm Edd}$ ($-2.67 < \log \lambda_{\rm Edd} < 0.00$), which excludes a small number of objects shown at both the high and low ends of $\lambda_{\rm Edd}$, and we found a significant correlation.

We further study the observed anticorrelation by looking for correlations with $M_{\rm BH}$ (Fig. 4). We find that [N II] λ6583/Hα, [S II] λλ6716, 6731/Hα, [O I] λ6300/Hα, and [O III] λ5007/Hβ show positive correlations with $M_{\rm BH}$, with p-values of 5×10^{-6}, 0.002 18, 0.000 09, and 0.001 74, respectively. In order to understand whether the anticorrelation of [N II] λ6583/Hα with $\lambda_{\rm Edd}$ is stronger than the correlation of [N II] λ6583/Hα with $M_{\rm BH}$, we run the z-test based on the two Pearson correlation coefficients and find that the p-value suggests a stronger anticorrelation for the $\lambda_{\rm Edd}$ (p-value = 0.025). We also investigate the observed anticorrelation between optical emission-line ratios and $\lambda_{\rm Edd}$ with fixed $M_{\rm BH}$ [$7 < \log (M_{\rm BH}/{\rm M}_\odot) < 8$, $8 < \log (M_{\rm BH}/{\rm M}_\odot) < 9$]. We find that [N II] λ6583/Hα is indeed significantly anticorrelated with $\lambda_{\rm Edd}$ in each of these mass bins, with p-values of 0.004 88 [$7 < \log (M_{\rm BH}/{\rm M}_\odot) < 8$] and 3×10^{-7} [$8 < \log (M_{\rm BH}/{\rm M}_\odot) < 9$]. On the other hand,

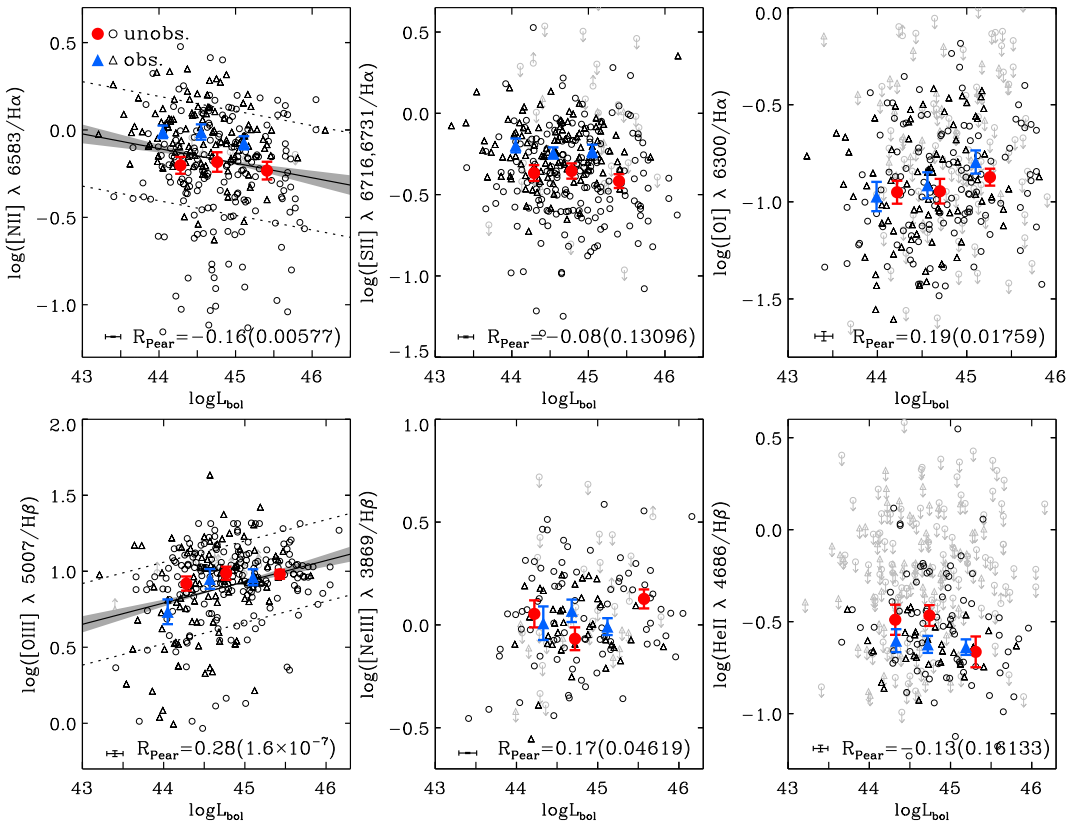

Figure 5. Optical emission-line ratio versus bolometric luminosity. The format is the same as that of Fig. 2.

the other line ratios do not show any correlation with $\lambda_{\rm Edd}$ at any fixed $M_{\rm BH}$, except [S II] λλ6716, 6731/Hα, which shows a p-value of 5×10^{-5} in a high-$M_{\rm BH}$ bin. We also test how the relationships between emission-line ratios and $M_{\rm BH}$ change at fixed $\lambda_{\rm Edd}$ ($-2.5 < \log \lambda_{\rm Edd} < -1.5$, $-1.5 < \log \lambda_{\rm Edd} < -0.5$). We find that [O I] λ6300/Hα and [O III] λ5007/Hβ show only a weak correlation at both fixed $\lambda_{\rm Edd}$ bins with a less than 1 per cent level of p-value.

Finally, we find a negative correlation with the $L_{\rm bol}$ (Fig. 5) for [N II] λ6583/Hα (p-value = 0.005 77), whereas a positive correlation is found for [O III] λ5007/Hβ (p-value $= 2 \times 10^{-6}$). Running the z-test based on the two Pearson correlation coefficients for [N II] λ6583/Hα with $\lambda_{\rm Edd}$ compared to [N II] λ6583/Hα with $L_{\rm bol}$ again suggests a statistically stronger correlation (p-value = 0.0001) in $\lambda_{\rm Edd}$. While [N II] λ6583/Hα shows correlations with $M_{\rm BH}$ and $L_{\rm bol}$, the correlation with $M_{\rm BH}$ is more significant at a less than 5 per cent level based on a Fisher z test (p-value = 0.036).

In order to understand the effect of the different bolometric corrections, we estimate $L_{\rm bol}$ and $\lambda_{\rm Edd}$ following Marconi et al. (2004), who uses bolometric corrections that depend on 2–10 keV luminosity (equation 21 in their paper). The mean difference between the newly estimated $L_{\rm bol}$ and the one derived by our prescription is 0.03 dex with 0.33 dex of scatter, which gives a mean difference in $\lambda_{\rm Edd}$ of 0.03 dex (0.33 dex of scatter). We find that [N II] λ6583/Hα (p-value $= 10^{-12}$) and [S II] λλ6716, 6731/Hα (p-value $= 1 \times 10^{-6}$) show a significant anticorrelation with $\lambda_{\rm Edd}$. If we adopt a more steep bolometric correction curve that varies with 2–10 keV luminosity (see fig. 3 in Marconi et al. 2004) covering a wide range of bolometric corrections, we may get a flattened relationship in [N II] λ6583/Hα and $\lambda_{\rm Edd}$ as sources in low $\lambda_{\rm Edd}$ and high $\lambda_{\rm Edd}$ move towards each end. However, we find that the application of such extreme cases of bolometric correction does not significantly change the Pearson R coefficient (−0.43) and p-value (10^{-12}) but shows a slightly moderate slope (-0.10 ± 0.01).

4 DISCUSSION

We have presented the observed relationship between the $\lambda_{\rm Edd}$ and optical emission-line ratios ([N II] λ6583/Hα, [S II] λλ6716, 6731/Hα, [O I] λ6300/Hα, [O III] λ5007/Hβ, [Ne III] λ3869/Hβ, and He II λ4686/Hβ) using local obscured and unobscured AGN ($\langle z \rangle = 0.05$, $z < 0.40$) from the 70-month *Swift*-BAT all-sky hard X-ray survey with follow-up optical spectroscopy. We show that there is a significant anticorrelation between the [N II] λ6583/Hα emission-line ratio and $\lambda_{\rm Edd}$, and this correlation is stronger than trends with $M_{\rm BH}$ or $L_{\rm bol}$ or with other line ratios. The observed trend suggests that optical emission-line ratios, which are widely used to classify sources as AGN, can also be an indicator of $\lambda_{\rm Edd}$. The use of [N II] λ6583 and Hα emission lines as a $\lambda_{\rm Edd}$ indicator has potential implications for high-redshift obscured AGN whose $M_{\rm BH}$ and $\lambda_{\rm Edd}$ are difficult to estimate. This would require an additional assumption that any relevant physical relations that might affect our $\lambda_{\rm Edd}$–[N II] λ6583/Hα relation (e.g. the stellar mass–metallicity, AGN outflows), do not evolve significantly with redshift. The relationship shown in this work may serve as a basis for future studies towards measuring $M_{\rm BH}$ and $\lambda_{\rm Edd}$ of individual AGN.

A number of complications arise when measuring $L_{\rm bol}$ and $M_{\rm BH}$ from a large ($N > 100$) sample of galaxies. The majority of the total luminosity is emitted from the accretion disc in the extreme-UV and UV energy bands (Shields 1978; Malkan & Sargent 1982; Mathews & Ferland 1987). While we used a fixed bolometric correction from the X-ray, this correction has been observed to vary

depending on $\lambda_{\rm Edd}$ (Vasudevan et al. 2009) and $L_{\rm bol}$ (e.g. Just et al. 2007; Green et al. 2009). This issue deserves further study, though we would expect any biases to affect all line ratios; we find a much stronger correlation with [N II] λ6583/Hα. Another complication is the use of separate methods of BH mass estimates. We note, however, that these two methods are tied to reproduce similar masses for systems where both are applicable (Graham et al. 2011; Woo et al. 2013), and that we find significant correlations for both type 1 and type 2 AGN separately (Table 1). We will explore $M_{\rm BH}$ measurements for both types of AGN via different methods in a future study.

There are several possible physical mechanisms that might lead to the trends found between $\lambda_{\rm Edd}$ and emission-line ratios such as [N II] λ6583/Hα. Groves, Heckman & Kauffmann (2006) and Stern & Laor (2013) found a dependence of emission-line diagnostics, particularly of [N II] λ6583/Hα, on host galaxy stellar mass. They postulated that this was a result of the mass–metallicity relationship with more massive galaxies having more metals (Lequeux et al. 1979; Tremonti et al. 2004; Erb et al. 2006; Lee et al. 2006; Ellison et al. 2008; Maiolino et al. 2008; Lara-López et al. 2010; Mannucci et al. 2010). As more massive galaxies have more massive black holes, this follows the correlation found here with [N II] λ6583/Hα being positively correlated with $M_{\rm BH}$ and negatively correlated with $L_{\rm bol}$. Stern & Laor (2013) showed that [O III] λ5007/Hβ mildly decreases with stellar mass since reduced [O III] λ5007 emission is expected from higher metallicity and massive systems as [O III] λ5007 is a main coolant and the temperature will be lower in massive systems. The less significant correlation between [O III] λ5007/Hβ and $M_{\rm BH}$ shown in Fig. 4 as compared to [N II] λ6583/Hα, which scales strongly with metallicity, can be explained in this context. Another interesting possibility affecting this correlation could be that higher $\lambda_{\rm Edd}$ AGN have relatively weaker [O III] λ5007 lines, as found by the 'Eigenvector 1' relationships (e.g. Boroson & Green 1992).

A further possibility is that X-ray heating induces some of the negative correlation found between $L_{\rm bol}$ and the [N II] λ6583/Hα ratio. Ionizing UV photons produce a highly ionized zone on the illuminated face of the gas cloud, whereas deeper in the cloud, penetrating X-rays heat the gas and maintain an extended partially ionized region. Higher energy photons such as Lyα are destroyed by multiple scatterings ending in collisional excitation, which enhances the Balmer lines (Weisheit, Tarter & Shields 1981; Krolik & Kallman 1983; Maloney, Hollenbach & Tielens 1996). Strong X-rays [i.e. harder spectral energy distributions (SEDs)] that heat up hot electrons in partially ionized regions also enhance the collisional excitation of O^0, N^+, and S^+. As a result, it is expected to see high [N II] λ6583/Hα, [S II] λλ6716, 6731/Hα, and [O I] λ6300/Hα.

Alternatively, the observed anticorrelation between emission-line ratios ([N II] λ6583/Hα and [S II] λλ6716, 6731/Hα) and $\lambda_{\rm Edd}$ may be due to radiatively driven outflows in high-$\lambda_{\rm Edd}$ systems. Radiatively accelerated wind is predicted to be proportional to $\lambda_{\rm Edd}$ (Shlosman, Vitello & Shaviv 1985; Arav, Li & Begelman 1994; Murray et al. 1995; Hamann 1998; Proga, Stone & Kallman 2000; Chelouche & Netzer 2001). This is consistent with the observed blueshift of broad as well as narrow absorption lines (Misawa et al. 2007) often seen in quasars. In the context of a prevalent outflow in high-$\lambda_{\rm Edd}$ AGN, the optical–UV SED of the accretion disc is expected to be softer when $\lambda_{\rm Edd} \gtrsim 0.3$ (King & Pounds 2003; Pounds et al. 2003; Reeves, O'Brien & Ward 2003; Tombesi et al. 2010, 2011; Slone & Netzer 2012; Veilleux et al. 2016; Woo et al. 2016). As hot accreting gas is removed by ejecting outflows, the formation of collisionally excited emission lines is expected to be suppressed. It is important to note, however, that the anticorrelation between optical emission-line ratio and $\lambda_{\rm Edd}$ appears only in [N II] λ6583/Hα and [S II] λλ6716, 6731/Hα but not in other line ratios.

5 SUMMARY

We present observed correlations between AGN Eddington ratio ($\lambda_{\rm Edd}$), black hole mass ($M_{\rm BH}$), and bolometric luminosity ($L_{\rm bol}$), and narrow-emission-line ratios ([N II] λ6583/Hα, [S II] λλ6716, 6731/Hα, [O I] λ6300/Hα, [O III] λ5007/Hβ, [Ne III] λ3869/Hβ, and He II λ4686/Hβ) for hard X-ray selected AGN from the BASS. The results of this study are as follows:

(i) $\lambda_{\rm Edd}$ is anticorrelated with both the [N II] λ6583/Hα and [S II] λλ6716, 6731/Hα ratios, but not with other line ratios.

(ii) [N II] λ6583/Hα exhibits a significantly stronger anticorrelation with $\lambda_{\rm Edd}$ than [S II] λλ6716, 6731/Hα.

(iii) The correlation shown in [N II] λ6583/Hα with $M_{\rm BH}$ is more significant than with $L_{\rm bol}$.

(iv) The correlation shown in [N II] λ6583/Hα with $M_{\rm BH}$ might be a result of the mass–metallicity relationship.

(v) The observed relationship between $\lambda_{\rm Edd}$ and the [N II] λ6583/Hα ratio could be explained by considering X-ray-heating processes and removal of material due to the energetic outflow in the high-$\lambda_{\rm Edd}$ state.

(vi) The [N II] λ6583/Hα ratio could, in principle, be used to measure accretion efficiencies and black hole masses of high-redshift obscured AGN (equation 2).

ACKNOWLEDGEMENTS

KO and KS acknowledge support from the Swiss National Science Foundation (SNSF) through Project grants 200021_157021, PP00P2_138979, and PP00P2_166159. MK acknowledges support from the SNSF through the Ambizione fellowship grant PZ00P2_154799/1. MK and KS acknowledge support from the SNFS through the Ambizione fellowship grant PP00P2 138979/1. CR acknowledges financial support from the CONICYT-Chile 'EMBIGGEN' Anillo (grant ACT1101), FONDECYT 1141218, Basal-CATA PFB–06/2007 and China-CONICYT fund. ET acknowledges support from the CONICYT-Chile 'EMBIGGEN' Anillo (grant ACT1101), FONDECYT 1160999, and Basal-CATA PFB–06/2007. The work of DS was carried out at the Jet Propulsion Laboratory, California Institute of Technology, under a contract with NASA. This research has made use of NASA's ADS Service.

Facilities: *Swift*, UH:2.2m, Sloan, KPNO:2.1m, FLWO:1.5m (FAST), Shane (Kast Double spectrograph), CTIO:1.5m, Hale, Gemini: South, Gemini: Gillett, Radcliffe, Perkins.

REFERENCES

Abazajian K. N. et al., 2009, ApJS, 182, 543
Alam S. et al., 2015, ApJS, 219, 12
Arav N., Li Z.-Y., Begelman M. C., 1994, ApJ, 432, 62
Baldwin J. A., Phillips M. M., Terlevich R., 1981, PASP, 93, 5
Barger A. J., Cowie L. L., Mushotzky R. F., Richards E. A., 2001, AJ, 121, 662
Barthelmy S. D. et al., 2005, Space Sci. Rev., 120, 143
Baumgartner W. H., Tueller J., Markwardt C. B., Skinner G. K., Barthelmy S., Mushotzky R. F., Evans P. A., Gehrels N., 2013, ApJS, 207, 19
Berney S. et al., 2015, MNRAS, 454, 3622
Boroson T. A., Green R. F., 1992, ApJS, 80, 109

Caccianiga A., Severgnini P., Della Ceca R., Maccacaro T., Carrera F. J., Page M. J., 2007, A&A, 470, 557
Campbell L. A. et al., 2014, MNRAS, 443, 1231
Cappellari M., Emsellem E., 2004, PASP, 116, 138
Chelouche D., Netzer H., 2001, MNRAS, 326, 916
Comastri A. et al., 2002, ApJ, 571, 771
Ellison S. L., Patton D. R., Simard L., McConnachie A. W., 2008, ApJ, 672, L107
Elvis M., Schreier E. J., Tonry J., Davis M., Huchra J. P., 1981, ApJ, 246, 20
Erb D. K., Shapley A. E., Pettini M., Steidel C. C., Reddy N. A., Adelberger K. L., 2006, ApJ, 644, 813
Gehrels N. et al., 2004, ApJ, 611, 1005
Graham A. W., Onken C. A., Athanassoula E., Combes F., 2011, MNRAS, 412, 2211
Green P. J. et al., 2009, ApJ, 690, 644
Greene J. E., Ho L. C., 2005, ApJ, 630, 122
Griffiths R. E., Georgantopoulos I., Boyle B. J., Stewart G. C., Shanks T., della Ceca R., 1995, MNRAS, 275, 77
Groves B. A., Heckman T. M., Kauffmann G., 2006, MNRAS, 371, 1559
Hamann F., 1998, ApJ, 500, 798
Harrison F. A. et al., 2013, ApJ, 770, 103
Iwasawa K., Koyama K., Awaki H., Kunieda H., Makishima K., Tsuru T., Ohashi T., Nakai N., 1993, ApJ, 409, 155
Jones D. H. et al., 2009, MNRAS, 399, 683
Just D. W., Brandt W. N., Shemmer O., Steffen A. T., Schneider D. P., Chartas G., Garmire G. P., 2007, ApJ, 665, 1004
Kauffmann G. et al., 2003, MNRAS, 346, 1055
Kelly B. C., 2007, ApJ, 665, 1489
Kewley L. J., Dopita M. A., Sutherland R. S., Heisler C. A., Trevena J., 2001, ApJ, 556, 121
Kewley L. J., Groves B., Kauffmann G., Heckman T., 2006, MNRAS, 372, 961
King A. R., Pounds K. A., 2003, MNRAS, 345, 657
Kormendy J., Ho L. C., 2013, ARA&A, 51, 511
Koss M. J. et al., 2016, ApJ, 825, 85
Krolik J. H., Kallman T. R., 1983, ApJ, 267, 610
Lara-López M. A. et al., 2010, A&A, 521, L53
Lee H., Skillman E. D., Cannon J. M., Jackson D. C., Gehrz R. D., Polomski E. F., Woodward C. E., 2006, ApJ, 647, 970
Lequeux J., Peimbert M., Rayo J. F., Serrano A., Torres-Peimbert S., 1979, A&A, 80, 155
Maiolino R., Salvati M., Bassani L., Dadina M., della Ceca R., Matt G., Risaliti G., Zamorani G., 1998, A&A, 338, 781
Maiolino R. et al., 2008, A&A, 488, 463
Malkan M. A., Sargent W. L. W., 1982, ApJ, 254, 22
Maloney P. R., Hollenbach D. J., Tielens A. G. G. M., 1996, ApJ, 466, 561
Mannucci F., Cresci G., Maiolino R., Marconi A., Gnerucci A., 2010, MNRAS, 408, 2115
Marconi A., Risaliti G., Gilli R., Hunt L. K., Maiolino R., Salvati M., 2004, MNRAS, 351, 169
Massaro E., Giommi P., Leto C., Marchegiani P., Maselli A., Perri M., Piranomonte S., Sclavi S., 2009, A&A, 495, 691
Mathews W. G., Ferland G. J., 1987, ApJ, 323, 456
Misawa T., Charlton J. C., Eracleous M., Ganguly R., Tytler D., Kirkman D., Suzuki N., Lubin D., 2007, ApJS, 171, 1
Murray N., Chiang J., Grossman S. A., Voit G. M., 1995, ApJ, 451, 498
Mushotzky R. F., Done C., Pounds K. A., 1993, ARA&A, 31, 717
Oh K., Sarzi M., Schawinski K., Yi S. K., 2011, ApJS, 195, 13
Oh K., Yi S. K., Schawinski K., Koss M., Trakhtenbrot B., Soto K., 2015, ApJS, 219, 1
Pounds K. A., King A. R., Page K. L., O'Brien P. T., 2003, MNRAS, 346, 1025
Proga D., Stone J. M., Kallman T. R., 2000, ApJ, 543, 686
Reeves J. N., O'Brien P. T., Ward M. J., 2003, ApJ, 593, L65
Reyes R. et al., 2008, AJ, 136, 2373
Ricci C., Ueda Y., Koss M. J., Trakhtenbrot B., Bauer F. E., Gandhi P., 2015, ApJ, 815, L13
Rigby J. R., Rieke G. H., Donley J. L., Alonso-Herrero A., Pérez-González P. G., 2006, ApJ, 645, 115
Rigby J. R., Diamond-Stanic A. M., Aniano G., 2009, ApJ, 700, 1878
Sarzi M. et al., 2006, MNRAS, 366, 1151
Schawinski K., Thomas D., Sarzi M., Maraston C., Kaviraj S., Joo S.-J., Yi S. K., Silk J., 2007, MNRAS, 382, 1415
Schawinski K., Koss M., Berney S., Sartori L. F., 2015, MNRAS, 451, 2517
Shields G. A., 1978, Nat, 272, 706
Shlosman I., Vitello P. A., Shaviv G., 1985, ApJ, 294, 96
Slone O., Netzer H., 2012, MNRAS, 426, 656
Stern J., Laor A., 2013, MNRAS, 431, 836
Tombesi F., Cappi M., Reeves J. N., Palumbo G. G. C., Yaqoob T., Braito V., Dadina M., 2010, A&A, 521, A57
Tombesi F., Cappi M., Reeves J. N., Palumbo G. G. C., Braito V., Dadina M., 2011, ApJ, 742, 44
Trakhtenbrot B., Netzer H., 2012, MNRAS, 427, 3081
Tremonti C. A. et al., 2004, ApJ, 613, 898
Vasudevan R. V., Mushotzky R. F., Winter L. M., Fabian A. C., 2009, MNRAS, 399, 1553
Veilleux S., Osterbrock D. E., 1987, ApJS, 63, 295
Veilleux S., Meléndez M., Tripp T. M., Hamann F., Rupke D. S. N., 2016, ApJ, 825, 42
Weisheit J. C., Tarter C. B., Shields G. A., 1981, ApJ, 245, 406
Winkler C. et al., 2003, A&A, 411, L1
Woo J.-H., Schulze A., Park D., Kang W.-R., Kim S. C., Riechers D. A., 2013, ApJ, 772, 49
Woo J.-H., Bae H.-J., Son D., Karouzos M., 2016, ApJ, 817, 108
Yuan S., Strauss M. A., Zakamska N. L., 2016, MNRAS, 462, 1603

This paper has been typeset from a TEX/LATEX file prepared by the author.